

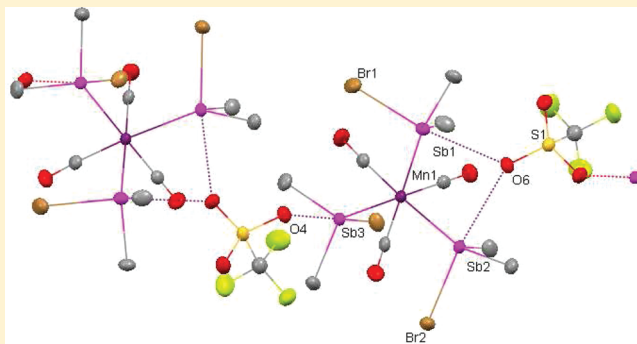
Halostibines  $\text{SbMeX}_2$  and  $\text{SbMe}_2\text{X}$ : Lewis Acids or Lewis Bases?

Sophie L. Benjamin, William Levason, Gillian Reid,\* and Robert P. Warr

School of Chemistry, University of Southampton, Southampton, U.K. SO17 1BJ

## Supporting Information

**ABSTRACT:** Alkylhalostibines have been shown to behave either as Lewis acids toward appropriate neutral ligands or as Lewis bases to low-valent metal fragments. The boundaries of their Lewis acid and Lewis base behavior have been determined, and the structural and spectroscopic consequences of the different behaviors probed.  $[\text{SbMeX}_2(\text{L-L})]$  ( $\text{L-L} = 2,2'$ -bipyridyl, 1,10-phenanthroline) and  $[\text{SbMeX}_2(\text{L})_2]$  ( $\text{L} = \text{OPMe}_3, \text{OPPh}_3$ ) are five-coordinate, distorted square-pyramidal monomers with the Me group axial, with the bond distances little affected by coordination. Significant changes in the bonding within the group 6 carbonyl complexes  $[\text{M}(\text{CO})_5(\text{L}')] ]$  are evident, with  $\text{L}' \rightarrow \text{M}$   $\sigma$ -donation decreasing across the series  $\text{L}' = \text{SbMe}_3 \rightarrow \text{SbMe}_2\text{Br} \rightarrow \text{SbMeBr}_2$ , and an increase in  $\text{M} \rightarrow \text{L}'$   $\pi$ -acceptance within the same series. Intermolecular interactions are a major feature within these systems, ranging from weak,  $\text{MCO} \cdots \text{Sb}$  interactions in  $[\text{M}(\text{CO})_5(\text{SbMe}_2\text{Br})]$  and  $[\text{M}(\text{CO})_5(\text{SbMeBr}_2)]$  to remarkably strong  $\text{O} \cdots \text{Sb}$  hypervalent bonds in  $[\text{Mn}(\text{CO})_5(\text{SbMe}_2\text{Br})][\text{CF}_3\text{SO}_3]$  and  $[\text{Mn}(\text{CO})_3(\text{SbMe}_2\text{Br})_3][\text{CF}_3\text{SO}_3]$ , the latter involving the triflate anions. These lead to large changes in the geometry at Sb and represent very rare examples in which the antimony exhibits significant Lewis acid and Lewis base behavior simultaneously. The coordinated alkylhalostibines are alkylated cleanly with MeLi or  ${}^n\text{BuLi}$ .



## INTRODUCTION

Stibines,  $\text{SbR}_3$ , and derivatives thereof have gained increasing importance in recent years for a number of reasons, most of which concern the realization that their chemistry is significantly different from that of the lighter group 15 phosphine and arsine analogues.<sup>1,2</sup> Triorganostibines utilize the antimony-based lone pair to function as modest Lewis bases toward a wide range of d- and p-block acceptors in medium or low oxidation states. Toward electron-rich d-block metals in low oxidation states they also exhibit weak  $\pi$ -acceptor ability ( $\text{M}(\text{d}\pi) \rightarrow \text{Sb}-\text{C}(\sigma^*)$ ).<sup>1</sup> Arguably the most important recent contribution to stibine chemistry has come from Werner and co-workers, who prepared the first examples of bridging  $\text{ER}_3$  ( $\text{E} = \text{P}, \text{As}, \text{Sb}$ ) ligands with  $\text{Sb}^{\text{I}}\text{Pr}_3$  (akin to bridging CO) and who showed that metathesis with  $\text{PR}_3$  or  $\text{AsR}_3$  also led to examples of these as bridging ligands, although the latter complexes cannot be obtained directly.<sup>3</sup> Theoretical studies have been used to probe the bonding in the bridging  $\text{ER}_3$  ligands.<sup>4</sup> Although little studied,  $\text{SbY}_3$  and  $\text{SbR}_{3-n}\text{Y}_n$  ( $\text{Y} = \text{GeR}_3, \text{SnR}_3, \text{NR}_2, \text{OR}, \text{SR}, \text{etc.}$ ), where the organic R groups are partially or wholly replaced by other substituents from groups 14–16, are also weak Lewis bases toward transition metal carbonyls and low-valent organometallics.<sup>5</sup> In marked contrast, while they retain the antimony-based lone pair, antimony(III) halides,  $\text{SbX}_3$  ( $\text{X} = \text{F}, \text{Cl}, \text{Br}, \text{or I}$ ), behave as moderately strong Lewis acids<sup>6</sup> toward a wide range of neutral N-,<sup>7</sup> P- or As-,<sup>8</sup> O-,<sup>9</sup> S-, or Se<sup>10</sup>-donor ligands, as well as forming a range of haloanions with  $\text{X}^-$ .<sup>6</sup> The reaction of  $\text{SbR}_3$  with  $\text{SbX}_3$  usually

results in scrambling to  $\text{SbR}_{3-n}\text{X}_n$  ( $n = 1$  or  $2$ ),<sup>11,12</sup> but at least one (unstable) adduct,  $[\text{Sb}_2\text{I}_6(\text{SbMe}_3)_2(\text{thf})_2]$ , is known.<sup>13</sup>

The major objective of the present work was to establish the boundaries of the Lewis acid to Lewis base behavior of the mixed alkylhalostibines,  $\text{SbMe}_2\text{Br}$  and  $\text{SbMeBr}_2$ , through detailed spectroscopic and structural measurements. This has allowed us to probe the consequences of the different behavior on the antimony center, especially the nature of their bonding toward either neutral donor ligands or transition metal centers. Few examples are available for compounds of this type. Lewis acid adducts include  $[\text{SbMeCl}_2(2,2'\text{-bipy})]$ ,<sup>14</sup>  $[\text{SbPhX}_2(2,2'\text{-bipy})]$ ,  $[\text{SbPhX}_2(\text{py})_n]$  ( $n = 1$  or  $2$ ), and  $[\text{SbPh}_2\text{X}(2,2'\text{-bipy})]$ .<sup>15</sup> Lewis base behavior is found in  $[\text{Cr}(\text{CO})_5(\text{SbMeCl}_2)]$ ,<sup>16</sup> in  $[\text{W}(\text{CO})_5(\text{SbPh}_2\text{X})]$  ( $\text{X} = \text{Cl}, \text{Br}, \text{or I}$ ),<sup>17</sup> and in the unique example of a bidentate halostibine in  $[\text{Rh}\{\text{Ph}_2\text{Sb}(\text{CH}_2)_3\text{SbPh}_2\}\{\text{PhClSb}(\text{CH}_2)_3\text{SbClPh}\}\text{Cl}_2]\text{Cl}$ .<sup>18</sup>

A further important phenomenon in organo-antimony chemistry that clearly distinguishes it from organo-phosphorus chemistry is the occurrence of hypervalency. For example,  $\text{SbR}_3$  (and  $\text{BiR}_3$ ) compounds can form significant interactions with adjacent electron donor groups (amines, ethers, etc.).<sup>19</sup> The extent of these interactions can lead to unexpected and potentially useful differences in reactivity, e.g., increasing the efficiencies and rates of Pd-catalyzed cross-coupling reactions.<sup>20</sup> In our recent work we have developed a range of new,

Received: November 9, 2011

Published: January 13, 2012

potentially tridentate,  $\text{Sb}_2\text{E}$  (and  $\text{Bi}_2\text{E}$ )-donor ligands ( $\text{E} = \text{O}, \text{S}, \text{NMe}$ ) and shown that varying degrees of hypervalent  $\text{E} \rightarrow \text{Sb}(\text{Bi})$  contacts occur both in the ligands themselves and also within their transition metal complexes.<sup>21</sup> We also anticipated that hypervalency might be evident in the chemistry of alkylhalostibines, and this would contribute to our understanding of this important and currently very active area of heavy p-block chemistry (*vide infra*). Finally, metal-coordinated alkylhalostibines may provide templates for the construction of polydentate and macrocyclic stibine ligands, very few examples of which are known.<sup>1,22</sup>

## RESULTS AND DISCUSSION

**Halostibines as Lewis Acids.** Complexes with phosphine oxides ( $\text{OPR}_3$ ,  $\text{R} = \text{Me}$  or  $\text{Ph}$ ) and the N-heterocycles 2,2'-bipyridyl and 1,10-phenanthroline were examined, the ligands being chosen since there are comparator data on  $\text{SbX}_3$  adducts available.<sup>7,9</sup> Reaction of the methylhalostibine  $\text{SbMeBr}_2$  with  $\text{OPPh}_3$  or  $\text{OPMe}_3$  in anhydrous MeCN resulted in formation of the 1:2 complexes  $[\text{SbMeBr}_2(\text{OPPh}_3)_2]$  and  $[\text{SbMeBr}_2(\text{OPMe}_3)_2]$  as white, powdered solids. Refrigeration of the filtrates gave the complexes as colorless crystals. Attempts to form analogous complexes with the dimethylhalostibines  $\text{SbMe}_2\text{X}$  were unsuccessful; the *in situ*  $^1\text{H}$  NMR spectrum of a mixture of  $\text{OPMe}_3$  and the  $\text{SbMe}_2\text{Br}$  showed no evidence of interaction. Slow crystallization from a mixture of  $\text{SbMe}_2\text{Cl}$  and  $\text{OPPh}_3$  in acetonitrile deposited crystals identified as  $[\text{SbMeCl}_2(\text{OPPh}_3)_2]$  (in 46% isolated yield), formed by disproportionation (see below). The structures of  $\text{SbMeCl}_2$  and  $\text{SbMeBr}_2$ <sup>16</sup> are both polymeric, based upon a pyramidal ( $\text{SbCX}_2$ ) core, linked into very distorted square pyramids with apical Me groups, by two further long  $\text{Sb}-\text{X}$  bonds in the basal plane, although the chain structure differs between the two compounds. In the phosphine oxide complexes the two  $\text{OPR}_3$  ligands are disposed *cis* and replace the longer  $\text{Sb}-\text{X}$  bonds (Figure 1–3). In both  $[\text{SbMeX}_2(\text{OPPh}_3)_2]$  species the axial Me

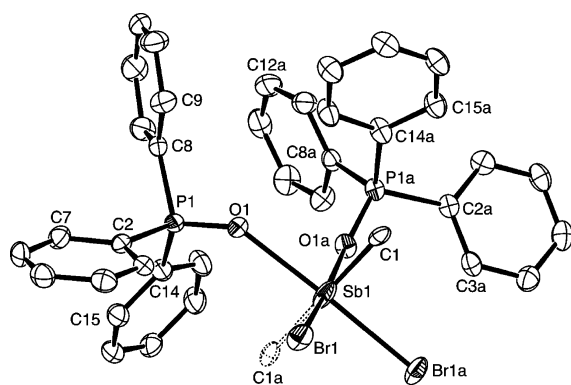


**Figure 1.** View of the structure of  $[\text{SbMeBr}_2(\text{OPPh}_3)_2]$  with atom-numbering scheme. Ellipsoids are shown at the 50% probability level, and H atoms are omitted for clarity. Symmetry operation:  $a = 1-x, y, 1/2-z$ . Note that the Me substituent on Sb1 is disordered over two sites; hence only one can be present in a given molecule. The alternative position is shown by the dotted bonds. Selected bond lengths (Å) and angles (deg):  $\text{Sb1}-\text{C1} = 1.947(7)$ ,  $\text{Sb1}-\text{O1} = 2.440(2)$ ,  $\text{Sb1}-\text{Br1} = 2.6675(5)$ ,  $\text{P1}-\text{O1} = 1.508(2)$ ;  $\text{C1}-\text{Sb1}-\text{O1a} = 86.2(2)$ ,  $\text{C1}-\text{Sb1}-\text{O1} = 94.1(2)$ ,  $\text{O1}-\text{Sb1}-\text{O1a} = 85.33(11)$ ,  $\text{C1}-\text{Sb1}-\text{Br1a} = 89.8(2)$ ,  $\text{O1}-\text{Sb1}-\text{Br1a} = 174.31(6)$ ,  $\text{C1}-\text{Sb1}-\text{Br1} = 89.9(2)$ ,  $\text{O1}-\text{Sb1}-\text{Br1} = 90.80(6)$ ,  $\text{Br1}-\text{Sb1}-\text{Br1a} = 93.35(2)$ .

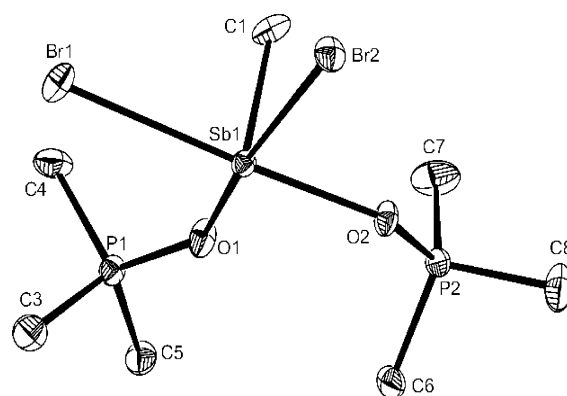


**Figure 2.** View of the structure of  $[\text{SbMeBr}_2(\text{OPMe}_3)_2]$  with atom-numbering scheme. Ellipsoids are shown at the 50% probability level, and H atoms are omitted for clarity. Selected bond lengths (Å) and angles (deg):  $\text{Sb1}-\text{C1} = 2.120(7)$ ,  $\text{Sb1}-\text{O1} = 2.235(4)$ ,  $\text{Sb1}-\text{O2} = 2.203(4)$ ,  $\text{Sb1}-\text{Br1} = 2.8370(9)$ ,  $\text{Sb1}-\text{Br2} = 2.8344(8)$ ,  $\text{Sb2}-\text{C2} = 2.128(7)$ ,  $\text{Sb2}-\text{O3} = 2.261(5)$ ,  $\text{Sb2}-\text{O4} = 2.244(5)$ ,  $\text{Sb2}-\text{Br3} = 2.8072(9)$ ,  $\text{Sb2}-\text{Br4} = 2.8133(8)$ ,  $\text{P1}-\text{O1} = 1.524(5)$ ,  $\text{P2}-\text{O2} = 1.527(5)$ ,  $\text{P3}-\text{O3} = 1.524(5)$ ,  $\text{P4}-\text{O4} = 1.524(5)$ ;  $\text{C1}-\text{Sb1}-\text{O1} = 86.8(2)$ ,  $\text{C1}-\text{Sb1}-\text{O2} = 88.1(2)$ ,  $\text{O1}-\text{Sb1}-\text{O2} = 83.1(2)$ ,  $\text{C1}-\text{Sb1}-\text{Br2} = 84.7(2)$ ,  $\text{O1}-\text{Sb1}-\text{Br2} = 167.72(12)$ ,  $\text{O2}-\text{Sb1}-\text{Br2} = 87.71(12)$ ,  $\text{C1}-\text{Sb1}-\text{Br1} = 85.6(2)$ ,  $\text{O1}-\text{Sb1}-\text{Br1} = 91.25(12)$ ,  $\text{O2}-\text{Sb1}-\text{Br1} = 171.79(12)$ ,  $\text{Br1}-\text{Sb1}-\text{Br2} = 96.97(3)$ ,  $\text{C2}-\text{Sb2}-\text{O3} = 85.2(2)$ ,  $\text{C2}-\text{Sb2}-\text{O4} = 87.7(2)$ ,  $\text{O3}-\text{Sb2}-\text{O4} = 83.9(2)$ ,  $\text{C2}-\text{Sb2}-\text{Br3} = 85.8(2)$ ,  $\text{O4}-\text{Sb2}-\text{Br3} = 172.88(12)$ ,  $\text{O3}-\text{Sb2}-\text{Br3} = 92.52(12)$ ,  $\text{C2}-\text{Sb2}-\text{Br4} = 85.3(2)$ ,  $\text{O3}-\text{Sb2}-\text{Br4} = 167.72(12)$ ,  $\text{O4}-\text{Sb2}-\text{Br4} = 87.90(12)$ .

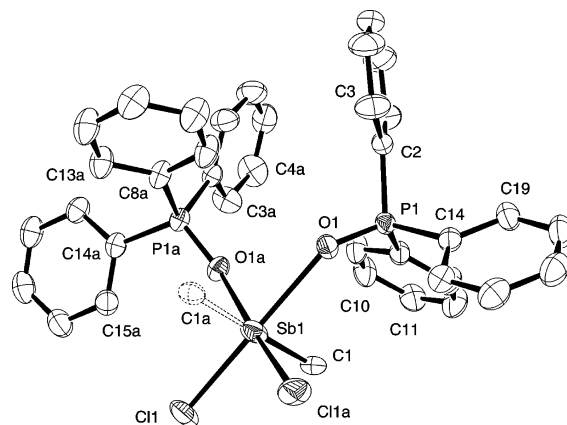


**Figure 3.** View of the structure of  $[\text{SbMeCl}_2(\text{OPPh}_3)_2]$  with atom-numbering scheme. Ellipsoids are shown at the 30% probability level, and H atoms are omitted for clarity. Symmetry operation:  $a = -x, y, 1/2-z$ . Note that the Me substituent on Sb1 is disordered over two sites (related by the crystallographic 2-fold axis); hence only one can be present in a given molecule. The alternative position is shown by the dotted bonds. Selected bond lengths (Å) and angles (deg):  $\text{Sb1}-\text{C1} = 1.941(6)$ ,  $\text{Sb1}-\text{O1} = 2.507(2)$ ,  $\text{Sb1}-\text{Cl1} = 2.5167(9)$ ,  $\text{P1}-\text{O1} = 1.503(2)$ ;  $\text{C1}-\text{Sb1}-\text{O1a} = 91.4(2)$ ,  $\text{C1}-\text{Sb1}-\text{O1} = 87.3(2)$ ,  $\text{O1}-\text{Sb1}-\text{O1a} = 84.74(10)$ ,  $\text{C1}-\text{Sb1}-\text{Cl1a} = 92.2(2)$ ,  $\text{C1}-\text{Sb1}-\text{Cl1} = 89.0(2)$ ,  $\text{O1}-\text{Sb1}-\text{Cl1} = 174.32(6)$ ,  $\text{O1}-\text{Sb1}-\text{Cl1a} = 91.05(6)$ ,  $\text{P1}-\text{O1}-\text{Sb1} = 141.27(12)$ ,  $\text{C1}-\text{Sb1}-\text{Cl1} = 92.17(18)$ .

group is disordered over two sites, and this disorder results in an unreasonably short  $\text{Sb}-\text{C}$  distance in each, accompanying elongated Sb ellipsoids along the  $\text{C}-\text{Sb}-\text{C}$  axis.  $[\text{SbMeBr}_2(\text{OPMe}_3)_2]$  has two molecules in the asymmetric unit, each of which shows the Sb atom displaced below the plane by an average of 0.170 Å in the direction opposite of the axial C.

The Sb–X distances in the OPR<sub>3</sub> adducts are longer than the corresponding distances in the parent SbMeX<sub>2</sub> (Sb–Cl = 2.392(2)–2.442(3) Å; Sb–Br = 2.564(3), 2.583(3) Å),<sup>16</sup> suggesting a rather stronger interaction with the *trans* phosphine oxide than in the secondary bonding to bridging halides in SbMeX<sub>2</sub>. The Sb–CH<sub>3</sub> in SbMeX<sub>2</sub> (2.129(7) Å, X = Cl; 2.301(9) Å, X = Br) compare with 2.120(7) and 2.128(7) Å in [SbMeBr<sub>2</sub>(OPMe<sub>3</sub>)<sub>2</sub>]. Comparison of the angles at antimony with those in the parent SbMeX<sub>2</sub><sup>16</sup> show that while ∠X–Sb–X are little changed, ∠C–Sb–X become more acute on formation of the phosphine oxide adducts, in the OPMe<sub>3</sub> complex by ~7°, and by much less than in the OPPh<sub>3</sub> analogues. Square-pyramidal coordination with *cis* basal OPPh<sub>3</sub> groups is also present in [SbCl<sub>3</sub>(OPPh<sub>3</sub>)<sub>2</sub>]<sup>23</sup> (Sb–Cl = 2.211(2), 2.466(1) Å). The Sb–O(P) distances are [SbMeBr<sub>2</sub>(OPPh<sub>3</sub>)<sub>2</sub>] 2.440(2), [SbMeCl<sub>2</sub>(OPPh<sub>3</sub>)<sub>2</sub>] 2.507(2), [SbCl<sub>3</sub>(OPPh<sub>3</sub>)<sub>2</sub>]<sup>23</sup> 2.455(2), and [SbMeBr<sub>2</sub>(OPMe<sub>3</sub>)<sub>2</sub>] 2.203(4)–2.261(5) Å. The IR spectra show modest low-frequency shifts in ν(PO) on complexation, similar to those found in SbX<sub>3</sub> (X = F, Cl, Br) adducts.<sup>9</sup>

The solution spectroscopic data show small high-frequency shifts in the <sup>1</sup>H, <sup>13</sup>C{<sup>1</sup>H}, and <sup>31</sup>P{<sup>1</sup>H} NMR resonances of the OPMe<sub>3</sub> groups on coordination, again similar to the corresponding SbX<sub>3</sub> adducts,<sup>9</sup> and since these complexes are expected to be labile and undergoing fast dissociative ligand exchange in solution at ambient temperatures, detailed numerical comparisons are not appropriate. In contrast, the <sup>1</sup>H resonances of the SbMe groups are little changed from those in SbMeX<sub>2</sub>.<sup>11</sup>

Three complexes with N-donor chelates [SbMeX<sub>2</sub>(1,10-phenanthroline)] (X = Cl or Br) and [SbMeBr<sub>2</sub>(2,2'-bipyridyl)] were prepared as yellow powders from reaction of the constituents in dry acetonitrile solution. Refrigeration of the filtrates from the syntheses gave crystalline samples used for the structure determinations. [SbMeCl<sub>2</sub>(2,2'-bipyridyl)] has been described previously by Althaus et al.,<sup>14</sup> and its structure determined. The reaction of SbMe<sub>2</sub>Br with 1,10-phenanthroline in MeCN gave an intensely orange solution, which over the course of ~30 min paled and deposited a yellow precipitate. The precipitate was identified as [SbMeBr<sub>2</sub>(1,10-phenanthroline)] by spectroscopic comparison with a genuine sample. Attempts to isolate the first, deeply colored product by working up the reaction immediately after mixing or by using low temperatures were unsuccessful, producing mixtures of starting materials, [SbMeBr<sub>2</sub>(1,10-phenanthroline)], and an unstable orange-red solid. The last is assumed to be [SbMe<sub>2</sub>Br(1,10-phenanthroline)], which is too unstable to separate and disproportionates into the yellow [SbMeBr<sub>2</sub>(1,10-phenanthroline)] and SbMe<sub>3</sub>. The SbMe<sub>3</sub> was identified *in situ* by its characteristic <sup>1</sup>H NMR resonance.

The structures of the four [SbMeX<sub>2</sub>(diimine)] complexes are similar (Figures 4–6), discrete square-pyramidal molecules with no contacts to neighboring molecules within the sum of the van der Waals radii. In each, the antimony lies slightly below the base plane and the strong σ-donor Me group is axial. Compared to SbMeX<sub>2</sub> both the Sb–C and Sb–X bond lengths have increased, probably reflecting the increase in coordination number to five, from a pyramidal three-coordinate core with two weaker secondary Sb–X bonds to neighboring molecules in SbMeX<sub>2</sub>. The small chelate bite angles of the diimines result in an acute ∠N–Sb–N of ~70°, but correspondingly the ∠X–Sb–X have opened up by 10–15° compared to SbMeX<sub>2</sub>. The symmetrical Sb–N coordination contrasts with the often disparate Sb–N bond lengths found in structures of these

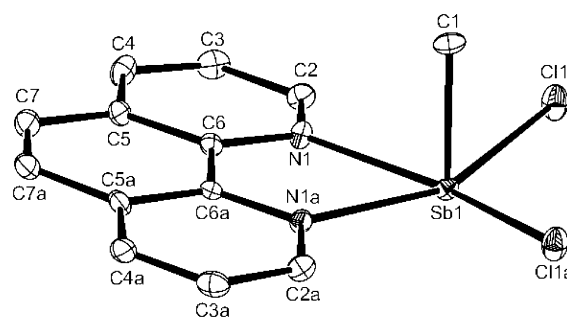


**Figure 4.** View of the structure of [SbMeCl<sub>2</sub>(1,10-phen)] with atom-numbering scheme. Ellipsoids are shown at the 50% probability level, and H atoms are omitted for clarity. Symmetry operation:  $a = x, 3/2 - y, z$ . Selected bond lengths (Å) and angles (deg): Sb1–C1 = 2.133(8), Sb1–N1 = 2.376(4), Sb1–Cl1 = 2.6534(14); C1–Sb1–N1 = 86.9(2), N1–Sb1–N1a = 69.9(2), C1–Sb1–Cl1 = 84.64(13), N1–Sb1–Cl1 = 87.40(12), N1–Sb1–Cl1a = 156.20(11), Cl1–Sb1–Cl1a = 113.83(6).

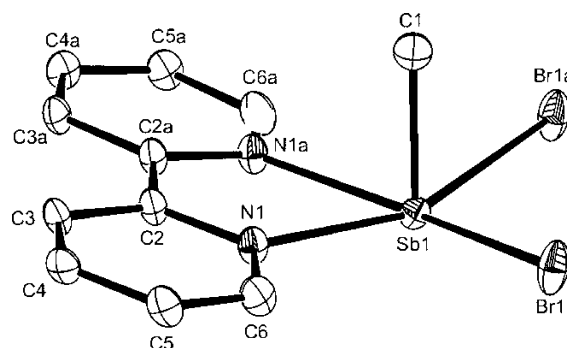


**Figure 5.** View of the structure of [SbMeBr<sub>2</sub>(2,2'-bipy)] with atom-numbering scheme. Ellipsoids are shown at the 50% probability level, and H atoms are omitted for clarity. Symmetry operation:  $a = x, 1/2 - y, z$ . Selected bond lengths (Å) and angles (deg): Sb1–C1 = 2.117(8), Sb1–N1 = 2.365(5), Sb1–Br1 = 2.7999(7), C1–Sb1–N1 = 85.2(2), N1–Sb1–N1a = 69.2(2), C1–Sb1–Br1 = 84.56(2), N1–Sb1–Br1 = 91.44(12), N1–Sb1–Br1a = 158.82(12), Br1–Sb1–Br1a = 106.01(3).

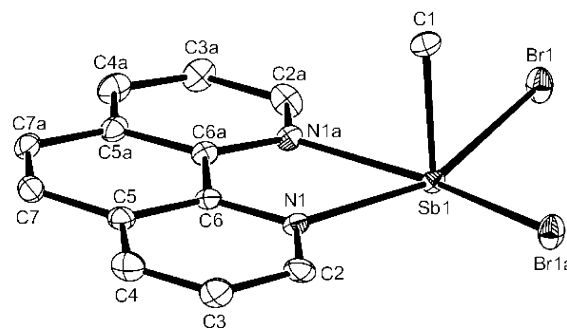


**Figure 6.** View of the structure of [SbMeBr<sub>2</sub>(1,10-phen)] with atom-numbering scheme. Ellipsoids are shown at the 50% probability level, and H atoms are omitted for clarity. Symmetry operation:  $a = x, -y, z$ . Selected bond lengths (Å) and angles (deg): Sb1–C1 = 2.120(4), Sb1–N1 = 2.377(3), Sb1–Br1 = 2.8138(5), C1–Sb1–N1 = 86.76(12), N1–Sb1–N1a = 70.23(12), C1–Sb1–Br1 = 84.91(7), N1–Sb1–Br1a = 88.46(6), N1–Sb1–Br1 = 157.52(6), C1–Sb1–Br1a = 84.90(7), Br1–Sb1–Br1a = 111.48(2).

two ligands with SbX<sub>3</sub> acceptors,<sup>7,24</sup> which seem to have no simple rationalization.

**Halostibines as Lewis Bases.** Both methylhalo- and dimethylhalo-stibines function as Lewis bases toward group 6

Table 1. Selected Spectroscopic and Structural Data

complex	$\nu(\text{CO})/\text{cm}^{-1}$ ( $\text{CH}_2\text{Cl}_2$ solution)	$\nu(\text{CO})/\text{cm}^{-1}$ Nujol mull	$\delta(\text{CO})$ $^{13}\text{C}\{^1\text{H}\}$ NMR	$d(\text{M}-\text{Sb})/\text{\AA}$
$[\text{W}(\text{CO})_5(\text{SbMe}_2\text{Br})]$	2085, 2005, 1966	2084, 1978, 1965, 1934	194.5, 196.6	2.6969(6)
$[\text{W}(\text{CO})_5(\text{SbMe}_2\text{Br})]$	2078, 1996, 1951	2077, 1993, 1962, 1953	195.6, 198.3	2.7186(4) to 2.7309(4)
$[\text{W}(\text{CO})_5(\text{SbMe}_3)]$	2068, 1972, 1940 <sup>a</sup>	2068, 1938, 1909 <sup>b</sup>	197.1, 199.7 <sup>a</sup>	2.759(1) <sup>b</sup>
$[\text{Cr}(\text{CO})_5(\text{SbMe}_2\text{Br})]^c$	not reported	2076, 1982, 1964	not reported	2.556(1)
$[\text{Cr}(\text{CO})_5(\text{SbMe}_2\text{Br})]$	2068, 1996, 1951	2069, 1991, 1966, 1952	215.9, 221.8	2.574(2)
$[\text{Cr}(\text{CO})_5(\text{SbMe}_3)]^b$	not reported	2069, 1940	218.3, 223.6	2.611(1)

<sup>a</sup>This work. <sup>b</sup>Data from ref 25. <sup>c</sup>Data from ref 16.

carbonyl residues, affording  $[\text{M}(\text{CO})_5\text{L}]$  complexes. However, attempted reaction of  $\text{SbBr}_3$  with  $[\text{W}(\text{CO})_5(\text{thf})]$  failed, only decomposition products being observed. The precursors  $[\text{M}(\text{CO})_5(\text{thf})]$  ( $\text{M} = \text{Cr}, \text{W}$ ), generated by photolysis of  $\text{M}(\text{CO})_6$  in thf, react with  $\text{SbMe}_2\text{Br}$  to give the air-stable complexes  $[\text{M}(\text{CO})_5(\text{SbMe}_2\text{Br})]$ . Similarly, treatment of  $[\text{W}(\text{CO})_5(\text{thf})]$  with  $\text{SbMeBr}_2$  results in formation of  $[\text{W}(\text{CO})_5(\text{SbMeBr}_2)]$ . The analogous chromium complex  $[\text{Cr}(\text{CO})_5(\text{SbMeBr}_2)]$  has been reported previously.<sup>16</sup> In chloro-carbon solutions these complexes show three carbonyl stretching vibrations in the IR spectra, as expected for a  $\text{C}_{4v}$  fragment (theory  $2a_1 + e$ ) (the asymmetry of alkylhalostibine ligands does not lead to observable splitting). Data are listed in Table 1 along with literature data on related complexes of  $\text{SbMe}_3$ . In the solid state several of the complexes show splitting of the carbonyl vibrations due to intermolecular interactions, discussed below when the crystal structures are described.

The  $^1\text{H}$  and  $^{13}\text{C}\{^1\text{H}\}$  NMR data show significant high-frequency shifts in the  $\delta(\text{Me})$  resonances on coordination to metal carbonyl residues, which contrasts with their behavior as Lewis acids (above), where no appreciable changes occurred. Considering the IR data, it is clear that  $\nu(\text{CO})$  generally fall along the series  $[\text{M}(\text{CO})_5(\text{SbMe}_2\text{Br})] \rightarrow [\text{M}(\text{CO})_5(\text{SbMe}_2\text{Br})] \rightarrow [\text{M}(\text{CO})_5(\text{SbMe}_3)]$ , consistent with higher electron density in the  $\text{CO } \pi^*$  orbitals along the series, which corresponds to higher electron density on the metal center in the same order. This could result either from greater  $\sigma$ -donation or reduced  $\pi$ -acceptance (or a combination of the two). The  $^{13}\text{C}\{^1\text{H}\}$  NMR data show the two resonances typical of a  $\text{C}_{4v}$  pentacarbonyl unit, and the shift to high frequency  $[\text{M}(\text{CO})_5(\text{SbMe}_2\text{Br})] \rightarrow [\text{M}(\text{CO})_5(\text{SbMe}_2\text{Br})] \rightarrow [\text{M}(\text{CO})_5(\text{SbMe}_3)]$  leads to the same conclusions as drawn from the IR spectroscopic data.<sup>26</sup>

The X-ray structures of  $[\text{W}(\text{CO})_5(\text{SbMe}_2\text{Br})]$ ,  $[\text{Cr}(\text{CO})_5(\text{SbMe}_2\text{Br})]$ , and  $[\text{W}(\text{CO})_5(\text{SbMe}_2\text{Br})]$  are shown in Figures 7–9; the structure of  $[\text{Cr}(\text{CO})_5(\text{SbMe}_2\text{Br})]$  has been reported by Breunig.<sup>16</sup> It is well established that on coordination of a triorganostibine to a metal center, the  $\angle\text{C}-\text{Sb}-\text{C}$  widen significantly, as the essentially  $\text{Sb } p^3$  character in the  $\text{Sb}-\text{C}$  bonds in the stibine changes toward  $\text{sp}^3$  in the metal complex, which improves the directional properties and strength of the  $\text{Sb}-\text{M}$  bond.<sup>1,27,28</sup> Similar effects are not generally found in  $\text{P}-\text{M}$  bonds in metal phosphine complexes and have their origin in the greater  $s-p$  orbital energy separations at antimony.  $\text{SbMe}_2\text{Br}$  is an oil at ambient temperatures, and no structural data are available. However, when  $\text{SbMeBr}_2$ , which has  $\angle\text{C}-\text{Sb}-\text{Br} = 91.2(2)^\circ, 92.6(2)^\circ$  and  $\angle\text{Br}-\text{Sb}-\text{Br} = 97.6(1)^\circ$ , coordinates in  $[\text{W}(\text{CO})_5(\text{SbMe}_2\text{Br})]$ , the angles open to  $\angle\text{C}-\text{Sb}-\text{Br} = 96.9(2)^\circ, 96.5(2)^\circ$  and  $\angle\text{Br}-\text{Sb}-\text{Br} = 98.9(1)^\circ$ , and similar trends are seen in  $[\text{Cr}(\text{CO})_5(\text{SbMe}_2\text{Br})]$ .<sup>16</sup> This widening of the angles at Sb is thus similar to that in triorganostibines, but contrasts with the contraction found in the

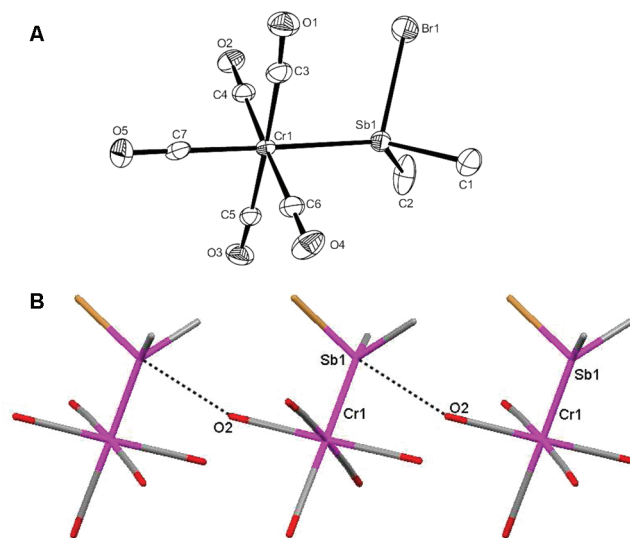


**Figure 7.** (a) View of the structure of  $[\text{Cr}(\text{CO})_5(\text{SbMe}_2\text{Br})]$  with atom-numbering scheme. Ellipsoids are shown at the 50% probability level, and H atoms are omitted for clarity. Selected bond lengths ( $\text{\AA}$ ) and angles (deg):  $\text{Cr1}-\text{C3} = 1.882(9)$ ,  $\text{Cr1}-\text{C4} = 1.899(9)$ ,  $\text{Cr1}-\text{C5} = 1.907(9)$ ,  $\text{Cr1}-\text{C6} = 1.905(9)$ ,  $\text{Cr1}-\text{C7} = 1.864(9)$ ,  $\text{Cr1}-\text{Sb1} = 2.5736(15)$ ,  $\text{Sb1}-\text{Br1} = 2.5239(13)$ ;  $\text{Br1}-\text{Sb1}-\text{Cr1}$ ,  $108.42(5)$ . (b) View of the packing in  $[\text{Cr}(\text{CO})_5(\text{SbMe}_2\text{Br})]$  showing the intermolecular  $(\text{C})\text{O}\cdots\text{Sb}$  interactions

Lewis acid adducts (above), the latter reflecting the increase in coordination number at Sb as well as electronic effects. Within the essentially square-pyramidal  $\text{M}(\text{CO})_5$  units, the  $\text{M}-\text{C}(\text{O})_{\text{transSb}}$  are typically shorter than  $\text{M}-\text{C}(\text{O})_{\text{transC}}$ , but the major feature of interest is the trend in  $\text{M}-\text{Sb}$  bonds (Table 1). Along the two series of tungsten and chromium complexes there is a clear lengthening of the  $\text{M}-\text{Sb}$  bond as  $\text{CH}_3$  replaces Br in the ligands. Combining this observation with the IR and  $^{13}\text{C}\{^1\text{H}\}$  NMR spectroscopic data discussed above leads to the conclusion that the key component must be an increase in  $\pi$ -acceptance by Sb as the number of Br substituents is increased, which shortens the  $\text{M}-\text{Sb}$  bond, but also leads to reduced electron density at M and in the carbonyl  $\pi^*$  orbitals.

Examination of the packing of the  $[\text{W}(\text{CO})_5(\text{SbMe}_2\text{Br})]$  molecules shows three intermolecular  $\text{Sb}\cdots\text{O}$  contacts ( $3.367-3.426 \text{ \AA}$ ) between the  $\text{SbMe}_2\text{Br}$  and carbonyl groups within the sum of the van der Waals radii ( $3.52 \text{ \AA}$ ) that lead to a “double-chain” arrangement in the crystal lattice (Figure 8).<sup>29</sup> Similar  $\text{Sb}\cdots\text{O}$  contacts are present between adjacent molecules in the structures of  $[\text{Cr}(\text{CO})_5(\text{SbMe}_2\text{Br})]$ ,  $[\text{W}(\text{CO})_5(\text{SbMe}_2\text{Br})]$ , and  $[\text{Cr}(\text{CO})_5(\text{SbMeBr}_2)]$ , although in these compounds these lead to infinite “single-chain” polymers (Figure 7b and Supporting Information) and although clearly weak, they are

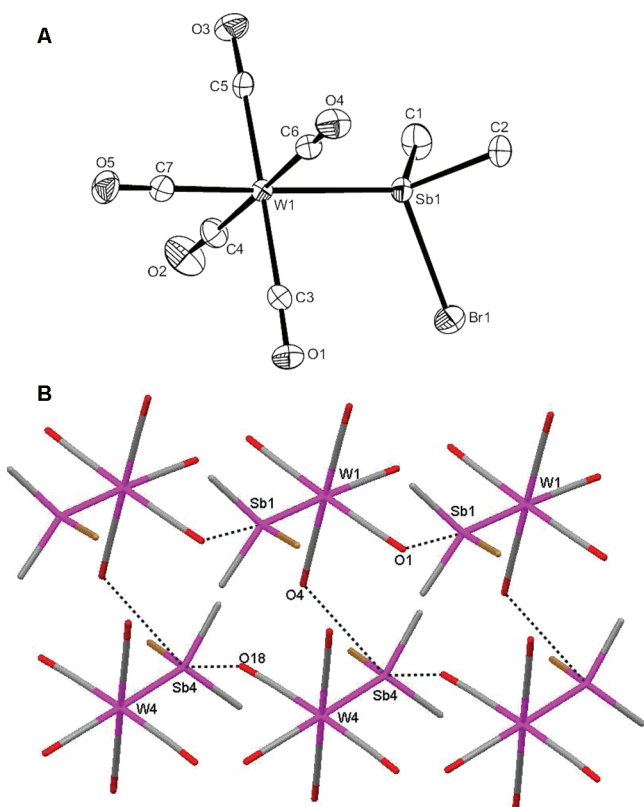


**Figure 8.** (a) View of the structure of  $[\text{W}(\text{CO})_5(\text{SbMe}_2\text{Br})]$  with atom-numbering scheme. Ellipsoids are shown at the 50% probability level, and H atoms are omitted for clarity. Selected bond lengths (Å) and angles (deg):  $\text{W1-Sb1} = 2.7280(4)$ ,  $\text{W2-Sb2} = 2.7186(4)$ ,  $\text{W3-Sb3} = 2.7247(4)$ ,  $\text{W4-Sb4} = 2.7309(4)$ ,  $\text{Sb1-Br1} = 2.5089(6)$ ,  $\text{Sb2-Br2} = 2.5121(7)$ ,  $\text{Sb3-Br3} = 2.5144(7)$ ,  $\text{Sb4-Br4} = 2.5148(6)$ ;  $\text{Br1-Sb1-W1} = 112.49(2)$ ,  $\text{Br2-Sb2-W2} = 111.24(2)$ ,  $\text{Br3-Sb3-W3} = 111.12(2)$ ,  $\text{Br4-Sb4-W4} = 111.41(2)$ . (b) View of the structure of  $[\text{W}(\text{CO})_5(\text{SbMe}_2\text{Br})]$  showing the “double-chain” arrangement formed through intermolecular  $(\text{C})\text{O}\cdots\text{Sb}$  interactions.

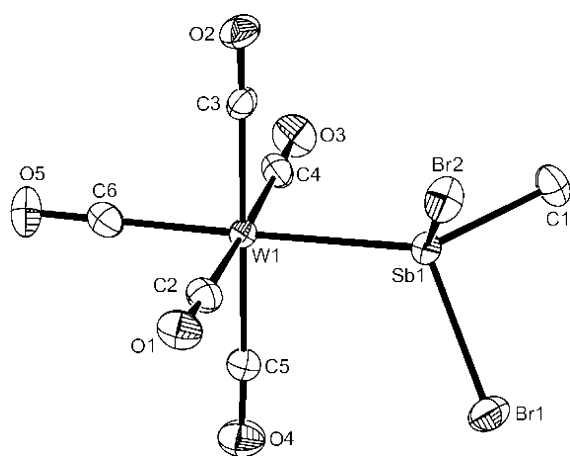


**Figure 9.** View of the structure of  $[\text{W}(\text{CO})_5(\text{SbMeBr}_2)]$  with atom-numbering scheme. Ellipsoids are shown at the 50% probability level, and H atoms are omitted for clarity. Note that the intermolecular  $(\text{C})\text{O}\cdots\text{Sb}$  contacts give rise to a chain structure (see Supporting Information). Selected bond lengths (Å) and angles (deg):  $\text{W1-C2} = 2.032(6)$ ,  $\text{W1-C3} = 2.049(6)$ ,  $\text{W1-C4} = 2.071(6)$ ,  $\text{W1-C5} = 2.044(6)$ ,  $\text{W1-C6} = 2.002(6)$ ,  $\text{W1-Sb1} = 2.6969(6)$ ,  $\text{Sb1-C1} = 2.116(6)$ ,  $\text{Sb1-Br1} = 2.5031(8)$ ,  $\text{Sb1-Br2} = 2.5012(8)$ ;  $\text{C1-Sb1-Br1} = 96.5(2)$ ,  $\text{C1-Sb1-Br2} = 96.9(2)$ ,  $\text{Br1-Sb1-Br2} = 98.78(3)$ .

sufficient to account for the complex IR spectra in the solid state. Similar behavior has been noted in  $[\text{W}(\text{CO})_5(\text{SbPh}_2\text{X})]$  complexes.<sup>17</sup>

The reaction of  $\text{SbMe}_2\text{Br}$  and  $[\text{Mn}(\text{CO})_5(\text{CF}_3\text{SO}_3)]$  in anhydrous  $\text{CH}_2\text{Cl}_2$  produced yellow crystals of  $[\text{Mn}(\text{CO})_5(\text{SbMe}_2\text{Br})][\text{CF}_3\text{SO}_3]$ . The only comparable triorganostibine cation is  $[\text{Mn}(\text{CO})_5(\text{SbPh}_3)]^+$ ,<sup>30,31</sup> but the IR and NMR data (including the observation that the  $^{55}\text{Mn}$  quadrupole causes serious line broadening in the  $^1\text{H}$  and  $^{13}\text{C}\{^1\text{H}\}$  NMR spectra) are much as expected, although very detailed comparisons as drawn in group 6 are not possible here due to insufficient literature examples.

The structure (Figure 10) shows the expected square-pyramidal  $\text{Mn}(\text{CO})_5$  residue with the sixth site occupied by

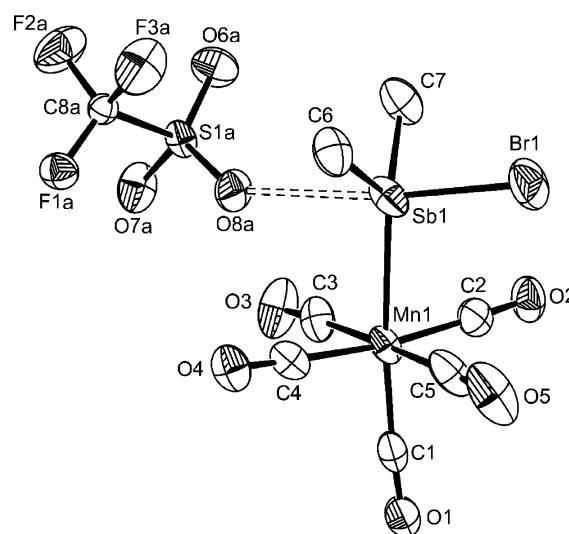


**Figure 10.** View of the structure of  $[\text{Mn}(\text{CO})_5(\text{SbMeBr}_2)][\text{CF}_3\text{SO}_3]$  with atom-numbering scheme, showing the long contact to  $\text{Sb1}$  via  $\text{O8a}$  of an adjacent  $[\text{CF}_3\text{SO}_3]^-$  anion. Ellipsoids are shown at the 50% probability level, and H atoms are omitted for clarity. Only one of the disordered  $\text{CF}_3\text{SO}_3^-$  anions is shown (the position of  $\text{O8a}$  is common to both). Symmetry operation:  $a = x, 1/2 - y, -1/2 + z$ . Selected bond lengths (Å) and angles (deg):  $\text{Mn1-C1} = 1.849(8)$ ,  $\text{Mn1-C2} = 1.870(8)$ ,  $\text{Mn1-C3} = 1.894(8)$ ,  $\text{Mn1-C4} = 1.887(7)$ ,  $\text{Mn1-C5} = 1.870(8)$ ,  $\text{Mn1-Sb1} = 2.5847(12)$ ,  $\text{Sb1-Br1} = 2.4933(11)$ ,  $\text{Sb1}\cdots\text{O8a} = 2.696(5)$ ;  $\text{C6-Sb1-C7} = 109.1(4)$ ,  $\text{C6-Sb1-Br1} = 94.6(2)$ ,  $\text{C7-Sb1-Br1} = 94.8(2)$ .

$\text{SbMe}_2\text{Br}$  ( $\text{Mn-Sb} = 2.5847(12)$  Å), which compares with  $2.596(3)$  Å in  $[\text{Mn}(\text{CO})_5(\text{SbPh}_3)]^+$ .<sup>31</sup> Most unusually, one of the O atoms of the triflate anion forms a strong hypervalent interaction with the coordinated Sb center ( $\text{O}\cdots\text{Sb} = 2.70$  Å), compared with the sum of the van der Waals radii of  $3.52$  Å.<sup>29</sup> The effect of this interaction is to severely distort the geometry at antimony, as evidenced by the  $\angle\text{Mn1-Sb1-Br1}$  angle of  $102.4^\circ$ , compared to  $125.9^\circ$  and  $120.0^\circ$  for  $\angle\text{Mn1-Sb1-C6}$  and  $\angle\text{Mn1-Sb1-C7}$ , respectively, and the wide  $\angle\text{C6-Sb1-C7} = 109.1(4)^\circ$ .

$[\text{Mn}(\text{CO})_3(\text{Me}_2\text{CO})_3][\text{CF}_3\text{SO}_3]$  in acetone solution reacted with  $\text{SbMe}_2\text{Br}$  to give the 3:1 complex  $[\text{Mn}(\text{CO})_3(\text{SbMe}_2\text{Br})_3][\text{CF}_3\text{SO}_3]$ , the first example of a transition metal coordinating three halostibine ligands; the key to the successful reaction is the lability of the weak donor acetone ligands. However, several attempts to prepare  $[\text{Mn}(\text{CO})_3(\text{SbMeBr}_2)_3][\text{CF}_3\text{SO}_3]$  were unsuccessful. The solution IR spectrum of  $[\text{Mn}(\text{CO})_3(\text{SbMe}_2\text{Br})_3][\text{CF}_3\text{SO}_3]$  shows one sharp and one broad  $\nu(\text{CO})$  band ( $a_1 + e$ ),

but again the IR spectrum obtained from a Nujol mull is more complicated due to intermolecular interactions (see below). The crystal structure (Figure 11) shows a pseudo-octahedral Mn center

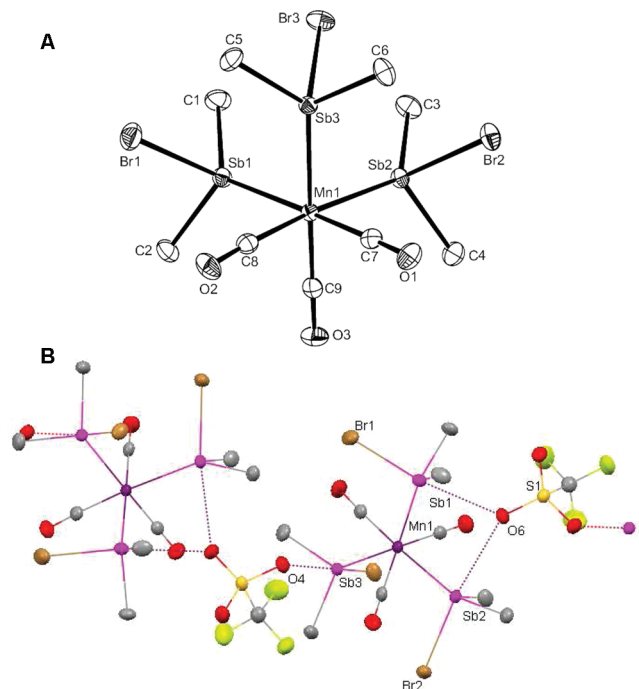


**Figure 11.** View of the structure of the  $[\text{Mn}(\text{CO})_3(\text{SbMe}_2\text{Br})_3]^+$  cation with atom-numbering scheme. Ellipsoids are shown at the 50% probability level, and H atoms are omitted for clarity. Selected bond lengths (Å) and angles (deg): Mn1–C9 = 1.814(3), Mn1–C8 = 1.825(3), Mn1–C7 = 1.835(3), Mn1–Sb1 = 2.5706(5), Mn1–Sb2 = 2.5852(5), Mn1–Sb3 = 2.5932(4), Sb1–Br1 = 2.5398(4), Sb2–Br2 = 2.5322(4), Sb3–Br3 = 2.5418(4), Sb1...O6 = 2.799(2), Sb2...O6 = 2.874(2), Sb3...O4a = 2.798(2); Sb1–Mn1–Sb2 = 93.646(15), Sb1–Mn1–Sb3 = 92.699(14), Sb2–Mn1–Sb3 = 93.863(15), Br1–Sb1–Mn1 = 107.191(14), Br2–Sb2–Mn1 = 107.956(14), Br3–Sb3–Mn1 = 105.471(13). (b) View of the packing within  $[\text{Mn}(\text{CO})_3(\text{SbMe}_2\text{Br})_3][\text{CF}_3\text{SO}_3]$  showing the hypervalent contacts between the O atoms of the  $[\text{CF}_3\text{SO}_3]^-$  anions and the Sb atoms of the cation.

in the cation. The Mn–Sb, Sb–Br, and Sb–C bond lengths are very similar to those in  $[\text{Mn}(\text{CO})_5(\text{SbMe}_2\text{Br})][\text{CF}_3\text{SO}_3]$  and contain hypervalent contacts from the triflate anions to the antimony, producing very distorted geometries. In this case, O6 from the triflate has short contacts with both Sb1 (2.80 Å) and Sb2 (2.87 Å), forming a puckered four-membered ring, while Sb3 interacts with O4 from the anion of the next unit (Sb...O4 = 2.80 Å), producing a polymeric chain structure as seen in Figure 11b. O5 from each anion has no interactions. These hypervalent Sb...O distances are significantly shorter, and the distortions in the antimony environment are greater than those we observed in metal carbonyl complexes of distibine ether ligands (which show intramolecular O→Sb hypervalency involving the ether function),<sup>21</sup> suggesting that the halostibines are much stronger acceptors toward the triflate oxygen donors than are triorganostibines toward ether oxygen.

Finally, species in which one or more halostibines are complexed to a transition metal could potentially be of use as reagents in the synthesis of more complex antimony ligands, by exploiting the reactivity of the antimony halide link with organolithium or Grignard reagents. As precursors, these complexes are far more stable than noncoordinated halostibines.

For example  $[\text{W}(\text{CO})_5(\text{SbMe}_2\text{Br})]$  is air-stable both as a solid and in solution, whereas  $\text{SbMe}_2\text{Br}$  is extremely air-sensitive and the neat oil disproportionates over time even in an inert atmosphere. Another possible advantage would be to use the central transition metal as a template to produce chelating polydentate (or macrocyclic) antimony ligands selectively. As proof-of-concept,  $[\text{W}(\text{CO})_5(\text{SbMe}_2\text{Br})]$  was treated with a stoichiometric amount of either MeLi in thf or  $^n\text{BuLi}$  in  $\text{Et}_2\text{O}$ . This resulted in formation of  $[\text{W}(\text{CO})_5(\text{SbMe}_3)]^{25}$  and  $[\text{W}(\text{CO})_5(\text{SbMe}_2^i\text{Bu})]$  in good yield, spectroscopically pure by IR and NMR, indicating clean substitution of the halide at the Sb center.

## EXPERIMENTAL SECTION

Infrared spectra were recorded as Nujol mulls between CsI plates using a Perkin-Elmer Spectrum 100 spectrometer over the range 4000–200  $\text{cm}^{-1}$ .  $^1\text{H}$  NMR spectra were recorded in  $\text{CDCl}_3$  or  $\text{CD}_2\text{Cl}_2$  unless otherwise stated, using a Bruker AV300 spectrometer.  $^{13}\text{C}\{^1\text{H}\}$ ,  $^{31}\text{P}\{^1\text{H}\}$ , and  $^{55}\text{Mn}$  NMR spectra were recorded using a Bruker DPX400 spectrometer and are referenced to the solvent resonance ( $^{13}\text{C}$ ), external 85%  $\text{H}_3\text{PO}_4$  ( $^{31}\text{P}$ ), and aqueous  $\text{KMnO}_4$  ( $^{55}\text{Mn}$ ). Microanalyses were undertaken by Medac Ltd. The  $\text{CH}_2\text{Cl}_2$  and acetonitrile were dried by distillation over  $\text{CaH}_2$ , while the toluene, benzene, THF, and *n*-hexane were dried over Na/benzophenone ketyl.  $\text{SbMe}_2\text{X}$  and  $\text{SbMeX}_2$  (X = Cl or Br) were made as described.<sup>32</sup> Antimony trihalides and all other reagents were obtained from Aldrich. The OPRs, 2,2'-bipy, and 1,10-phen were dried by heating *in vacuo* before use. All preparations were performed under an atmosphere of dry  $\text{N}_2$  using Schlenk techniques, and spectroscopic samples were prepared in a dry  $\text{N}_2$ -purged glovebox.  $\text{SbMePh}_2$ ,  $\text{SbMe}_2\text{Ph}$ ,<sup>32</sup>  $[\text{M}(\text{CO})_5(\text{thf})]$  (M = Cr or W),<sup>33</sup>  $[\text{Mn}(\text{CO})_5(\text{CF}_3\text{SO}_3)]$ ,<sup>30</sup> and  $[\text{Mn}(\text{CO})_5(\text{Me}_2\text{CO})_3][\text{CF}_3\text{SO}_3]$ <sup>30</sup> were prepared via the literature methods.

**SbMeBr<sub>2</sub>.**  $\text{SbMePh}_2$  (2.00 g, 6.87 mmol) was dissolved in toluene (80 mL), and HBr was bubbled through the solution for 15 min. The reaction vessel was sealed, and the reaction mixture was stirred for 30 min. Residual HBr was removed by passing a slow stream of nitrogen through the solution overnight. The solvent was removed *in vacuo*, yielding an off-white solid. Yield: 1.75 g, 86%.  $^1\text{H}$  NMR ( $\text{CDCl}_3$ ): 2.23 (s, Me); lit.<sup>12</sup> 2.2.  $^{13}\text{C}\{^1\text{H}\}$  NMR ( $\text{CDCl}_3$ ): 21.9 (Me).

**SbMeCl<sub>2</sub>.**  $\text{SbMePh}_2$  (2.00 g, 6.87 mmol) was dissolved in toluene (80 mL), and HCl was bubbled through the solution for 15 min. The reaction vessel was sealed, and the reaction mixture was stirred for 30 min. Residual HCl was removed by passing a slow stream of nitrogen through the solution overnight. The solvent was removed *in vacuo*, yielding an off-white solid. Yield: 1.00 g, 70%.  $^1\text{H}$  NMR ( $\text{CDCl}_3$ ): 1.88, (s, Me); lit.<sup>12</sup> 1.9.  $^{13}\text{C}\{^1\text{H}\}$  NMR ( $\text{CDCl}_3$ ): 27.5 (Me).

**SbMe<sub>2</sub>Br.**  $\text{SbMe}_2\text{Ph}$  (2.1 g, 9.2 mmol) was dissolved in benzene (100 mL), and HBr was bubbled through the solution for 15 min. The reaction vessel was sealed, and the reaction mixture was stirred for 30 min. Residual HBr was removed by passing a slow stream of nitrogen through the solution overnight. The solution was filtered, and the solvent was removed *in vacuo*, yielding a pale yellow oil. Yield: 1.2 g, 56%.  $^1\text{H}$  NMR ( $\text{CDCl}_3$ ): 1.49, (s, Me).  $^{13}\text{C}\{^1\text{H}\}$  NMR ( $\text{CDCl}_3$ ): 8.9 (Me).

**Halostibines As Lewis Acids.**  $[\text{SbMeBr}_2(\text{OPPh}_3)_2]$ .  $\text{SbMeBr}_2$  (0.14 g, 0.47 mmol) was added to a solution of  $\text{OPPh}_3$  (0.26 g, 0.94 mmol) in acetonitrile (12 mL). The reaction was stirred for 1 h, yielding a clear solution and white precipitate. The solid was isolated by filtration and dried *in vacuo*. Refrigeration of the filtrate (~16 h) gave colorless crystals, from which the X-ray data set was collected. Yield: 0.21 g, 52%. Anal. Calcd for  $\text{C}_{37}\text{H}_{33}\text{Br}_2\text{O}_2\text{P}_2\text{Sb}$  (853.2): C, 52.1; H, 3.9. Found: C, 51.9; H, 3.8. IR (Nujol/ $\text{cm}^{-1}$ ): 1133 (P=O).  $^1\text{H}$  NMR ( $\text{CDCl}_3$ ): 2.18 (s, [3H], MeSb), 7.4–7.7 (m, [30H], aromatics).  $^{31}\text{P}\{^1\text{H}\}$  NMR ( $\text{CDCl}_3$ ): 30.5.

**$[\text{SbMeBr}_2(\text{OPMe}_3)_2]$ .**  $\text{SbMeBr}_2$  (0.25 g, 0.85 mmol) was added to a solution of  $\text{OPMe}_3$  (0.17 g, 1.9 mmol) in acetonitrile (12 mL). The reaction was stirred for 1 h, resulting in a clear, colorless solution,

which was reduced *in vacuo* to ~5 mL, causing precipitation of a white solid, which was isolated by filtration and dried *in vacuo*. Refrigeration of the filtrate (~16 h) gave colorless crystals, from which the X-ray data set was collected. Yield: 0.23 g, 52%. Anal. Calcd for  $C_7H_{21}Br_2O_2P_2Sb$  (480.6): C, 17.5; H, 4.4. Found: C, 18.4; H, 4.5. IR (Nujol/ $cm^{-1}$ ): 1100(sh), 1085 (P=O).  $^1H$  NMR ( $CDCl_3$ ): 1.64 (d,  $^2J = 13.2$  Hz, [18H], MeP), 2.03 (s, [3H], MeSb).  $^{13}C\{^1H\}$  NMR ( $CDCl_3$ ): 18.4 (d,  $^1J = 74$  Hz, MeP), 29.8 (MeSb).  $^{31}P\{^1H\}$  NMR ( $CDCl_3$ ): 50.5.

**[SbMeCl<sub>2</sub>(OPPh<sub>3</sub>)<sub>2</sub>] from the Reaction of SbMe<sub>2</sub>Cl with OPPh<sub>3</sub>.** SbMe<sub>2</sub>Cl (0.17 g, 0.90 mmol) was added to a solution of OPPh<sub>3</sub> (0.50 g, 1.80 mmol) in acetonitrile (15 mL). The reaction was stirred for 1 h, resulting in a clear, colorless solution. The volume was reduced *in vacuo* to ~5 mL, and the solution refrigerated to yield colorless crystals identified by their X-ray structure. Yield: 0.15 g, 46% (based upon antimony). IR (Nujol/ $cm^{-1}$ ): 1136 (P=O).  $^1H$  NMR ( $CDCl_3$ ): 1.84 (s, [3H], MeSb), 7.4–7.7 (m, [30H], aromatics).  $^{13}C\{^1H\}$  NMR ( $CDCl_3$ ): 30.0 (MeSb), 129.3, 129.4, 132.8, 132.9, 133.0, and 133.1 (aromatics).  $^{31}P\{^1H\}$  NMR ( $CDCl_3$ ): 32.0.

**[SbMeBr<sub>2</sub>(2,2'-bipyridyl)].** SbMeBr<sub>2</sub> (0.25 g, 0.84 mmol) was added to a solution of 2,2'-bipyridyl (0.13 g, 0.84 mmol) in acetonitrile (10 mL). The reaction mixture was stirred for 1 h, resulting in a pale yellow solution and a yellow precipitate. The solid was isolated by filtration and dried *in vacuo*. Refrigeration of the filtrate (~16 h) gave yellow crystals, from which the X-ray data were collected. Yield: 0.23 g, 60%. Anal. Calcd for  $C_{11}H_{11}Br_2N_2Sb$  (542.8): C, 29.2; H, 2.5; N, 6.2. Found: C, 28.9; H, 2.7; N, 4.9.  $^1H$  NMR ( $CD_2Cl_2$ ): 1.86 (s, [3H], MeSb), 7.86 (t, [2H]), 8.19 (t, [2H]), 8.32 (d, [2H]), and 9.54 (d, [2H]) (aromatics).

**[SbMeBr<sub>2</sub>(1,10-phenanthroline)].** SbMeBr<sub>2</sub> (0.25 g, 0.84 mmol) was added to a solution of 1,10-phenanthroline (0.15 g, 0.84 mmol) in acetonitrile (10 mL). The reaction was stirred for 1 h, resulting in a yellow solution and yellow precipitate. The solid was isolated by filtration and dried *in vacuo*. Refrigeration of the filtrate (~16 h) gave yellow crystals. Yield: 0.27 g, 67%. Anal. Calcd for  $C_{13}H_{11}Br_2N_2Sb$  (476.8): C, 32.8; H, 2.3; N, 5.9. Found: C, 32.8; H, 2.3; N, 5.6.  $^1H$  NMR ( $CD_2Cl_2$ ): 1.96 (s, [3H], MeSb), 8.00 (m, [2H]), 8.11 (s, [2H]), 8.70 (d, [2H]), and 9.93 (d, [2H]) (aromatics).

**[SbMeCl<sub>2</sub>(1,10-phenanthroline)].** SbMeCl<sub>2</sub> (0.25 g, 1.2 mmol) was added to a solution of 1,10-phenanthroline (0.22 g, 1.2 mmol) in acetonitrile (12 mL). The reaction was stirred for 2 h, resulting in a yellow precipitate. The solid was isolated by filtration and dried *in vacuo*. Refrigeration of the filtrate (~16 h) gave yellow crystals. Yield: 0.38 g, 82%. Anal. Calcd for  $C_{13}H_{11}Cl_2N_2Sb$  (387.9): C, 40.3; H, 2.9; N, 7.2. Found: C, 39.9; H, 3.1; N, 6.5.  $^1H$  NMR ( $CD_2Cl_2$ ): 1.78 (s, [3H], MeSb), 7.99 (m, [2H]), 8.09 (s, [2H]), 8.63 (d, [2H]), and 9.82 (d, [2H]) (aromatics).

**Halostibines As Lewis Bases.** **[W(CO)<sub>5</sub>(SbMe<sub>2</sub>Br)].** A solution of  $W(CO)_6$  (0.30 g, 0.86 mmol) in thf (50 mL) was photolyzed for 1.25 h. The resulting yellow solution was added to a solution of SbMe<sub>2</sub>Br (0.20 g, 0.86 mmol) in thf (10 mL). The mixture was stirred for 3 h, after which the volatiles were removed *in vacuo* to yield a bright yellow solid. *n*-Hexane (40 mL) was added, and the resultant pale yellow solution stirred for 0.5 h, then filtered to remove some undissolved solids. The filtrate was reduced in volume to ~10 mL, causing precipitation of a pale yellow solid, which was isolated by filtration. Crystals grew from the filtrate at -18 °C, and these were used for the X-ray data collection. Yield: 0.19 g, 40%. Anal. Calcd for  $C_7H_6BrO_5SbW$  (555.6): C, 15.1; H, 1.1. Found: C, 14.7; H, 1.5. IR ( $CH_2Cl_2/cm^{-1}$ ): 2078m, 1996w, 1951vs, br; (Nujol/ $cm^{-1}$ ): 2077s, 1993w, 1962sh, 1953s.  $^1H$  NMR ( $CDCl_3$ ): 2.06 (s, SbMe).  $^{13}C\{^1H\}$  NMR ( $CDCl_3$ ): 12.3 (SbMe), 195.6 ( $^1J_{WC} = 118$  Hz, CO), 198.3 ( $^1J_{WC} = 162$  Hz, CO).

**[Cr(CO)<sub>5</sub>(SbMe<sub>2</sub>Br)].** The preparation was similar to that for  $[W(CO)_5(SbMe_2Br)]$ , from  $Cr(CO)_6$  (0.19 g, 0.86 mmol) and SbMe<sub>2</sub>Br (0.20 g, 0.86 mmol). Yellow crystals grew from the filtrate. Yield: 0.12 g, 33%. Anal. Calcd for  $C_7H_6BrCrO_5Sb$  (423.8): C, 19.8; H, 1.4. Found: C, 20.4; H, 1.5. IR ( $CH_2Cl_2/cm^{-1}$ ): 2068m, 1996w, 1951vs, br; (Nujol/ $cm^{-1}$ ): 2069s, 1991m, 1966m, 1952s.  $^1H$  NMR ( $CDCl_3$ ): 1.97 (s, SbMe).  $^{13}C\{^1H\}$  NMR ( $CDCl_3$ ): 12.1 (SbMe), 215.9 (CO), 221.8 (CO).

**[W(CO)<sub>5</sub>(SbMeBr<sub>2</sub>)].** A solution of  $W(CO)_6$  (0.24 g, 0.67 mmol) in thf (40 mL) was photolyzed for 1.25 h. The resulting solution was added to a solution of SbMeBr<sub>2</sub> (0.20 g, 0.67 mmol) in thf (10 mL). The mixture was stirred for 1 h, after which the volatiles were removed *in vacuo* to yield a bright yellow solid. *n*-Hexane (40 mL) was added, the resultant yellow-orange solution stirred for 30 min and filtered, and the filtrate reduced *in vacuo* to ~10 mL. The orange solid precipitate was isolated by filtration and dried *in vacuo*. Orange crystals grew from the filtrate at -18 °C and were used for the X-ray structure determination. Yield: 0.28 g, 64%. Anal. Calcd for  $C_6H_3Br_2O_5SbW$  (620.5): C, 11.6; H, 0.5. Found: C, 11.9; H, 1.2. IR ( $CH_2Cl_2/cm^{-1}$ ): 2085m, 2005w, 1966s, br; (Nujol/ $cm^{-1}$ ): 2084m, 1978sh, 1965sh, 1934m.  $^1H$  NMR ( $CDCl_3$ ): 2.73 (s, SbMe).  $^{13}C\{^1H\}$  NMR ( $CDCl_3$ ): 27.3 (SbMe), 194.5 ( $^1J_{WC} = 123$  Hz, CO), 196.6 ( $^1J_{WC} \approx 164$  Hz, CO).

**Reaction of [W(CO)<sub>5</sub>(SbMe<sub>2</sub>Br)] with MeLi.**  $[W(CO)_5(SbMe_2Br)]$  (0.12 g, 0.22 mmol) was dissolved in thf (30 mL) and cooled to -78 °C. MeLi (1.6 M in Et<sub>2</sub>O, 0.135 mL, 0.22 mmol) was added dropwise, and the mixture was stirred at -78 °C for 45 min, then allowed to warm very slowly to room temperature and stirred for 1 h. The volatiles were removed *in vacuo* to yield a yellow solid, identified as  $[W(CO)_5(SbMe_3)]$ . IR (Nujol/ $cm^{-1}$ ): 2067m, 1941s, 1903s. (lit.<sup>25</sup> 2068, 1938, 1901). IR ( $CH_2Cl_2/cm^{-1}$ ): 2068m, 1972w, 1935vs.  $^1H$  NMR ( $C_6D_6$ ): 0.56 (s, Me) (lit.<sup>21</sup> 0.56).  $^{13}C\{^1H\}$  NMR ( $C_6D_6$ ): 2.8 (Me), 197.1 (CO), 199.7 (CO) (lit.<sup>25</sup> 2.8, 197.1, 199.7).

**Reaction of [W(CO)<sub>5</sub>(SbMe<sub>2</sub>Br)] with <sup>n</sup>BuLi.**  $[W(CO)_5(SbMe_2Br)]$  (0.15 g, 0.3 mmol) was dissolved in diethyl ether (30 mL), and the resultant yellow solution cooled to -78 °C. <sup>n</sup>BuLi (0.19 mL of 1.6 M solution, 0.3 mmol) was added dropwise, and the reaction mixture was stirred for 45 min, then warmed to room temperature and stirred for 1 h. The resultant cloudy yellow solution was filtered over Celite to remove LiBr, then concentrated *in vacuo* to ~10 mL. Hexane (15 mL) was added, precipitating a pale yellow solid, which was isolated by filtration. IR ( $CH_2Cl_2/cm^{-1}$ ): 2068w, 1970sh, 1936s; (Nujol/ $cm^{-1}$ ): 2068w, 1939s.  $^1H$  NMR ( $CDCl_3$ ): 0.96 (t, [3H], Me), 1.24 (s, [6H], SbMe), 1.39 (m, [2H], CH<sub>2</sub>), 1.58 (m, [2H], CH<sub>2</sub>), 1.83 (m, [2H], CH<sub>2</sub>).  $^{13}C\{^1H\}$  NMR ( $CDCl_3$ ): -2.9 (SbMe), 13.9, 17.2, 25.9, and 28.9 (Sb<sup>n</sup>Bu), 197.2 and 200.0 (CO).

**[Mn(CO)<sub>5</sub>(SbMe<sub>2</sub>Br)][CF<sub>3</sub>SO<sub>3</sub>].**  $[Mn(CO)_5Br]$  (0.15 g, 0.54 mmol) and  $Ag[CF_3SO_3]$  (0.21 g, 0.81 mmol) were dissolved in  $CH_2Cl_2$  (20 mL). The reaction was stirred for 2 h in the absence of light, forming a yellow solution and an off-white solid, which was removed by filtration. The filtrate was added to a solution of SbMe<sub>2</sub>Br (0.25 g, 1.1 mmol) in  $CH_2Cl_2$  (5 mL) and stirred (~48 h), yielding a yellow solution, which was filtered to remove some solid impurities and reduced *in vacuo* to ~10 mL. Then *n*-hexane (10 mL) was added. This caused precipitation of a yellow solid, which was isolated by filtration and dried *in vacuo*. Refrigeration of the filtrate (~16 h) yielded yellow crystals, used for X-ray data collection. Yield: 0.2 g, 71%. Anal. Calcd for  $C_8H_6BrF_3MnO_5SSb$  (575.8): C, 16.7; H, 1.1. Found: C, 17.3; H, 1.2. IR (Nujol/ $cm^{-1}$ ): 2145 m, 2054s, br; ( $CH_2Cl_2/cm^{-1}$ ): 2138m, 2056s, 2042(sh).  $^1H$  NMR ( $CDCl_3$ ): 2.57 (s, Me).  $^{13}C\{^1H\}$  NMR ( $CDCl_3$ ): 17.3 (Me), 205 (br, CO).  $^{55}Mn$  NMR ( $CH_2Cl_2$ ): -1672 ( $w_{1/2} = 1400$  Hz).

**[Mn(CO)<sub>3</sub>(SbMe<sub>2</sub>Br)<sub>3</sub>][CF<sub>3</sub>SO<sub>3</sub>].**  $[Mn(CO)_5Br]$  (0.2 g, 0.73 mmol) and  $Ag[CF_3SO_3]$  (0.19 g, 0.73 mmol) were dissolved in acetone (30 mL), and the mixture was refluxed for 1 h, resulting in a yellow solution and a white solid, which was removed by filtration. The solvent from the filtrate was removed *in vacuo*, leaving a yellow oil, which was redissolved in  $CH_2Cl_2$  (20 mL), forming a yellow solution. A solution of SbMe<sub>2</sub>Br (2.18 mmol) in toluene (40 mL) was added, and the mixture stirred for 16 h. The volume was reduced *in vacuo* until a yellow precipitate formed, which was isolated by filtration and dried *in vacuo*. Refrigeration of the filtrate (3 d) gave small yellow crystals and a small amount of insoluble white decomposition product. Anal. Calcd for  $C_{10}H_{18}Br_3F_3MnO_6SSb_3$  (983.2): C, 12.2; H, 1.9. Found: C 12.3, H 1.3. IR (Nujol/ $cm^{-1}$ ): 2039s, 1984m, 1973s, 1969sh; ( $CH_2Cl_2/cm^{-1}$ ): 2040s, 1974s, br.  $^1H$  NMR ( $CDCl_3$ ): 2.37 (s, Me).  $^{13}C\{^1H\}$  NMR ( $CDCl_3$ ): 15.0 (Me), 224.7 (CO).  $^{55}Mn$  NMR ( $CH_2Cl_2$ ): -1381 ( $w_{1/2} = 450$  Hz).

Table 2. Crystal Data and Structure Refinement Details<sup>a</sup>

	[SbMeBr <sub>2</sub> (OPPh <sub>3</sub> ) <sub>2</sub> ]	[SbMeBr <sub>2</sub> (OPMe <sub>3</sub> ) <sub>2</sub> ]	[SbMeCl <sub>2</sub> (OPPh <sub>3</sub> ) <sub>2</sub> ]	[SbMeCl <sub>2</sub> - (1,10-phen)]	[SbMeBr <sub>2</sub> - (1,10-phen)]	[SbMeBr <sub>2</sub> - (2,2'-bipy)]
formula	C <sub>37</sub> H <sub>33</sub> Br <sub>2</sub> O <sub>2</sub> P <sub>2</sub> Sb	C <sub>7</sub> H <sub>21</sub> Br <sub>2</sub> O <sub>2</sub> P <sub>2</sub> Sb	C <sub>37</sub> H <sub>30</sub> Cl <sub>2</sub> O <sub>2</sub> P <sub>2</sub> Sb	C <sub>13</sub> H <sub>11</sub> Cl <sub>2</sub> N <sub>2</sub> Sb	C <sub>13</sub> H <sub>11</sub> Br <sub>2</sub> N <sub>2</sub> Sb	C <sub>11</sub> H <sub>11</sub> Br <sub>2</sub> N <sub>2</sub> Sb
M	853.14	480.75	761.20	387.89	476.81	452.79
cryst syst	monoclinic	monoclinic	monoclinic	monoclinic	monoclinic	monoclinic
space group	C2/c (no. 15)	P2 <sub>1</sub> /c (no. 14)	C2/c (no. 15)	P2 <sub>1</sub> /m (no. 11)	Cm (no. 8)	P2 <sub>1</sub> /m (no. 11)
a [Å]	17.128(4)	20.039(3)	17.307(3)	5.4428(5)	7.7806(15)	5.7015(10)
b [Å]	12.347(2)	9.235(2)	12.339(3)	15.996(3)	16.546(3)	16.459(3)
c [Å]	16.956(4)	19.831(4)	17.099(4)	7.7092(15)	5.5726(10)	7.0828(10)
α [deg]	90	90	90	90	90	90
β [deg]	104.979(10)	117.145(10)	104.664(15)	96.317(10)	98.455(10)	95.639(10)
γ [deg]	90	90	90	90	90	90
U [Å <sup>3</sup> ]	3464.1(12)	3265.8(11)	3532.6(13)	667.12(19)	709.6(2)	661.46(18)
Z	4	8	4	2	2	2
μ(Mo Kα) [mm <sup>-1</sup> ]	3.227	6.761	1.054	2.450	7.558	8.101
total no. reflns	19 016	37 437	25 941	8803	4534	11 179
unique reflns	3986	7450	4054	1565	1545	1574
R <sub>int</sub>	0.060	0.056	0.040	0.035	0.028	0.046
no. of params, restraints	205, 0	253, 0	204, 0	90, 4	91, 5	81, 4
R <sub>1</sub> <sup>b</sup> [I <sub>o</sub> > 2σ(I <sub>o</sub> )]	0.040	0.049	0.042	0.045	0.018	0.043
R <sub>1</sub> [all data]	0.050	0.059	0.054	0.046	0.018	0.047
wR <sub>2</sub> <sup>b</sup> [I <sub>o</sub> > 2σ(I <sub>o</sub> )]	0.094	0.101	0.103	0.107	0.041	0.105
wR <sub>2</sub> [all data]	0.099	0.104	0.111	0.107	0.041	0.107
	[Mn(CO) <sub>5</sub> (SbMe <sub>2</sub> Br) [CF <sub>3</sub> SO <sub>3</sub> ]]	[Mn(CO) <sub>5</sub> (SbMe <sub>2</sub> Br) <sub>3</sub> [CF <sub>3</sub> SO <sub>3</sub> ]-C <sub>6</sub> H <sub>5</sub> Me]		[Cr(CO) <sub>5</sub> (SbMe <sub>2</sub> Br)]	[W(CO) <sub>5</sub> (SbMe <sub>2</sub> Br)]	[W(CO) <sub>5</sub> (SbMe <sub>2</sub> Br)]
formula	C <sub>8</sub> H <sub>6</sub> BrF <sub>3</sub> MnO <sub>8</sub> Sb	C <sub>17</sub> H <sub>26</sub> Br <sub>3</sub> F <sub>3</sub> MnO <sub>6</sub> Sb <sub>3</sub>		C <sub>7</sub> H <sub>6</sub> BrCrO <sub>5</sub> Sb	C <sub>7</sub> H <sub>6</sub> BrO <sub>5</sub> SbW	C <sub>6</sub> H <sub>3</sub> Br <sub>2</sub> O <sub>5</sub> SbW
M	575.79	1075.36		423.78	555.63	620.50
cryst syst	monoclinic	monoclinic		monoclinic	triclinic	orthorhombic
space group	P2 <sub>1</sub> /c (no. 14)	P2 <sub>1</sub> /n (no. 14)		P2 <sub>1</sub> /c (no. 14)	P $\bar{1}$ (no. 2)	Pbca (no. 61)
a [Å]	13.023(2)	14.4226(5)		16.261(5)	6.6070(5)	6.5876(10)
b [Å]	7.6958(14)	14.6672(10)		6.488(5)	17.0844(15)	12.473(3)
c [Å]	16.455(3)	14.5421(10)		12.287(5)	24.302(2)	31.209(6)
α [deg]	90	90		90	105.828(4)	90
β [deg]	93.553(7)	102.658(3)		107.735(5)	96.329(4)	90
γ [deg]	90	90		90	97.999(5)	90
U [Å <sup>3</sup> ]	1646.0(5)	3001.5(3)		1234.7(11)	2581.7(4)	2564.4(8)
Z	4	4		4	8	8
μ(Mo Kα) [mm <sup>-1</sup> ]	5.026	7.193		6.300	14.089	17.300
total no. reflns	18 193	44 598		14 744	42 746	18 132
unique reflns	3727	6850		2377	11 817	2951
R <sub>int</sub>	0.034	0.039		0.060	0.039	0.043
no. of params, restraints	235, 0	308, 0		136, 0	541, 0	137, 0
R <sub>1</sub> <sup>b</sup> [I <sub>o</sub> > 2σ(I <sub>o</sub> )]	0.061	0.023		0.065	0.028	0.028
R <sub>1</sub> [all data]	0.0667	0.025		0.066	0.033	0.036
wR <sub>2</sub> <sup>b</sup> [I <sub>o</sub> > 2σ(I <sub>o</sub> )]	0.154	0.051		0.180	0.065	0.056
wR <sub>2</sub> [all data]	0.158	0.053		0.182	0.069	0.060

<sup>a</sup>Common items: temperature = 120 K; wavelength (Mo Kα) = 0.71073 Å; θ(max) = 27.5°. <sup>b</sup>R<sub>1</sub> =  $\sum ||F_o| - |F_c|| / \sum |F_o|$ . wR<sub>2</sub> =  $[\sum w(F_o^2 - F_c^2)^2 / \sum wF_o^4]^{1/2}$ .

**X-ray Crystallography.** Details of the crystallographic data collection and refinement parameters are given in Table 2. Crystals were obtained as described above. Data collection used a Nonius Kappa CCD diffractometer fitted with monochromated (confocal mirrors) Mo Kα X-radiation (λ = 0.71073 Å). Crystals were held at 120 K in a nitrogen gas stream. Structure solution and refinement were generally routine<sup>34,35</sup> except as described below, with hydrogen atoms on C were added to the model in calculated positions and using the default C–H distance. The structures of [SbMeX<sub>2</sub>(OPPh<sub>3</sub>)<sub>2</sub>] (X = Cl or Br) revealed the Me group to be disordered over two sites related by the crystallographic 2-fold axis, although this was modeled satisfactorily. For [SbMeX<sub>2</sub>(2,2'-bipyridyl)] (X = Cl, Br) the H atoms on the Me group were placed using AFIX 137. The Z value of 8 (Z' = 4) for

[W(CO)<sub>5</sub>(Me<sub>2</sub>BrSb)] was unexpected, but appears to be genuine, probably resulting from the long Sb...O intermolecular contacts (*vide supra*). The anion in [Mn(CO)<sub>5</sub>(SbMe<sub>2</sub>Br)][CF<sub>3</sub>SO<sub>3</sub>] is disordered and was modeled well as two overlapping half-occupancy triflates.

CCDC reference numbers 850439 to 850449 contain the supplementary crystallographic data for this paper. These data can be obtained free of charge from The Cambridge Crystallographic Data Centre via [www.ccdc.cam.ac.uk/data\\_request/cif](http://www.ccdc.cam.ac.uk/data_request/cif).

## CONCLUSIONS

This work has established that halostibines can behave as both Lewis acids and Lewis bases to appropriate neutral ligands and

to metal fragments, respectively. The boundaries of their Lewis acid and Lewis base behavior have been determined, and the structural consequences of the different behaviors probed. Spectroscopic and structural studies show that where they behave as Lewis acids, only small differences from the parent halostibine are observed, whereas their Lewis base behavior results in significant changes in the geometric parameters at Sb. The studies reveal that the bonding between the halostibine and transition metal carbonyl fragments varies significantly across the series  $\text{SbR}_3$ ,  $\text{SbR}_2\text{X}$ ,  $\text{SbRX}_2$ , showing that the anticipated decrease in  $\sigma$ -donation is accompanied by an unexpectedly large increase in  $\pi$ -acceptance as the number of X groups increases. Typically,  $\pi$ -acceptance in  $\text{SbR}_3$  systems is only ever modest (considerably less important than in  $\text{PR}_3$ ) due to the large orbital size and low electronegativity of the Sb atom.

Intermolecular interactions are clearly evident in the new metal carbonyl complexes, including both  $\text{M}\cdots\text{CO}\cdots\text{Sb}$  contacts (producing extended chain structures in the solid state) in the Group 6 pentacarbonyl complexes and surprisingly strong triflate  $\text{O}\cdots\text{Sb}$  bonds evident in the manganese complexes. The bond distances in the latter are approaching those of normal covalent bonds and lead to very significant distortions at the Sb atoms. This results in the antimony center functioning as an electron pair donor and acceptor (both Lewis acid and Lewis base) simultaneously, and such behavior may have important implications in the reaction chemistry of halostibine complexes.

The first example of three halostibines on a single metal center is reported and taken together with the clean alkylation of  $[\text{W}(\text{CO})_5(\text{SbMe}_2\text{Br})]$  to  $[\text{W}(\text{CO})_5(\text{SbMe}_2\text{R})]$  ( $\text{R} = \text{Me}$  or  $^t\text{Bu}$ ) using  $\text{MeLi}$  or  $^t\text{BuLi}$ , respectively, suggests that this chemistry may have potential for metal-templated routes to polystibines.

## ■ ASSOCIATED CONTENT

### Supporting Information

Cif files for the crystal structures described, together with packing diagrams showing the  $\text{Sb}\cdots\text{O}$  intermolecular contacts in  $[\text{W}(\text{CO})_5(\text{SbMe}_2\text{Br})]$  and  $[\text{Cr}(\text{CO})_5(\text{SbMe}_2\text{R})]$ . This material is available free of charge via the Internet at <http://pubs.acs.org>.

## ■ AUTHOR INFORMATION

### Corresponding Author

\*E-mail: [G.Reid@soton.ac.uk](mailto:G.Reid@soton.ac.uk)

## ■ ACKNOWLEDGMENTS

We thank the EPSRC for support (EP/F038763/1) and for a studentship (S.L.B.). We also thank Dr. M. Webster for assistance with the X-ray crystallographic studies.

## ■ REFERENCES

- (1) (a) Champness, N. R.; Levason, W. *Coord. Chem. Rev.* **1994**, *133*, 115. (b) Levason, W.; Reid, G. *Comprehensive Coordination Chemistry II*; McCleverty, J. A.; Meyer, T. J., Eds.; Elsevier 2004; Vol. 1, p 377. (c) Levason, W.; Reid, G. *Coord. Chem. Rev.* **2006**, *250*, 2565. (d) Stulz, S. *Coord. Chem. Rev.* **2001**, *1*, 215.
- (2) (a) Werner, H.; Ortmann, D. A.; Gevert, O. *Chem. Ber.* **1996**, *129*, 411. (b) Werner, H.; Grünwald, C.; Steinert, P.; Gevert, O.; Wolf, J. *J. Organomet. Chem.* **1998**, *565*, 231. (c) Manger, M.; Wolf, J.; Laubender, M.; Teichert, M.; Stalke, D.; Werner, H. *Chem.—Eur. J.* **1997**, *3*, 1442. (d) Bleuel, E.; Gevert, O.; Laubender, M.; Werner, H. *Organometallics* **2000**, *19*, 3109. (e) Ortmann, D. A.; Weberndörfer, B.;

- Schöneboom, J.; Werner, H. *Organometallics* **1999**, *18*, 952. (f) Ortmann, D. A.; Weberndörfer, B.; Ilg, K.; Laubender, M.; Werner, H. *Organometallics* **2002**, *21*, 2369. (g) Werner, H.; Schwab, P.; Heinemann, A.; Steinert, P. *J. Organomet. Chem.* **1995**, *496*, 207. (h) Ortmann, D. A.; Gevert, O.; Laubender, M.; Werner, H. *Organometallics* **2001**, *20*, 1776. (i) Yasuike, S.; Okajima, S.; Yamaguchi, K.; Kurita, J. *Tetrahedron Lett.* **2003**, *44*, 6217. (j) Yasuike, S.; Okajima, S.; Yamaguchi, K.; Seki, H.; Kurita, J. *Tetrahedron* **2003**, *59*, 4959. (k) Yasuike, S.; Okajima, S.; Yamaguchi, K.; Seki, H.; Kurita, J. *Tetrahedron: Asymmetry* **2000**, *11*, 4043. (l) Jimenez-Tenorio, M.; Puerta, M. C.; Salcedo, I.; Valerga, P.; Costa, S. I.; Gomes, P. T.; Mereiter, K. *Chem. Commun.* **2003**, 1168. (m) Jimenez-Tenorio, M.; Puerta, M. C.; Salcedo, I.; Valerga, P.; de los Rios, I.; Mereiter, K. *Dalton Trans.* **2009**, 1842. (n) Casares, J. A.; Espinet, P.; Martin-Alvarez, J. M.; Martinez-Illarduya, J. M.; Salas, G. *Eur. J. Inorg. Chem.* **2005**, 3825.

- (3) Werner, H. *Angew. Chem., Int. Ed.* **2004**, *43*, 938.
- (4) Schinzel, S.; Müller, R.; Riedel, S.; Werner, H.; Kaupp, M. *Chem.—Eur. J.* **2011**, *17*, 7228.
- (5) (a) Wieber, M.; Höhl, H.; Burschka, C. *Z. Anorg. Allg. Chem.* **1990**, *583*, 113. (b) Kiennemann, A.; Kieffer, R. *C. R. Acad. Sci., Ser. C* **1974**, *279*, 355. (c) Schumann, H. *J. Organomet. Chem.* **1986**, *299*, 169. (d) Brill, T. B. *J. Organomet. Chem.* **1972**, *40*, 373.
- (6) (a) Norman, N. C., Ed. *The Chemistry of Arsenic, Antimony and Bismuth*; Blackie: London, 1998; p 207. (b) Levason, W.; Reid, G. *Comprehensive Coordination Chemistry II*; McCleverty, J. A.; Meyer, T. J., Eds.; Elsevier: Oxford, 2004; Vol. 3, p 465.
- (7) Lead references: (a) Yin, H. D.; Zhai, J. *Inorg. Chim. Acta* **2009**, *362*, 339. (b) Willey, G. R.; Daly, L. T.; Meehan, P. R.; Drew, M. G. B. *J. Chem. Soc., Dalton Trans.* **1996**, 4045. (c) Benjamin, S. L.; Burt, J.; Levason, W.; Reid, G.; Webster, M. *J. Fluor. Chem.*, doi:10.1016/j.jfluchem.2011.09.007.
- (8) (a) Clegg, W.; Elsegood, M. R. J.; Norman, N. C.; Pickett, N. L. *J. Chem. Soc., Dalton Trans.* **1994**, 173. (b) Genge, A. R. J.; Hill, N. J.; Levason, W.; Reid, G. *J. Chem. Soc., Dalton Trans.* **2001**, 1007. (c) Clegg, W.; Elsegood, M. R. J.; Graham, V.; Norman, N. C.; Pickett, N. L. *J. Chem. Soc., Dalton Trans.* **1993**, 997.
- (9) (a) Milicev, S.; Hadzlj, D. *Inorg. Chim. Acta* **1977**, *21*, 201. (b) Alcock, N. W.; Nicholson, D. G.; Vasudevan, A. K. *J. Chem. Soc., Dalton Trans.* **1987**, 427. (c) Neuhaus, A.; Frenzen, G.; Pebler, J.; Dehnicke, K. *Z. Anorg. Allg. Chem.* **1992**, *31*, 334. (d) Levason, W.; Light, M. E.; Maheshwari, S.; Reid, G.; Zhang, W. *Dalton Trans.* **2011**, *40*, 5291.
- (10) (a) Barton, A. J.; Hill, N. J.; Levason, W.; Reid, G. *J. Chem. Soc., Dalton Trans.* **2001**, 1621. (b) Levason, W.; Maheshwari, S.; Ratnani, R.; Reid, G.; Webster, M.; Zhang, W. *Inorg. Chem.* **2010**, *49*, 9036.
- (11) Wieber, M. *Gmelin Handbook of Inorganic Chemistry, Sb Organic Compounds, Part 2*; Springer Verlag: New York, 1981.
- (12) Ates, M.; Breunig, H. J.; Gulec, S. *J. Organomet. Chem.* **1989**, *364*, 67.
- (13) Breunig, H. J.; Denker, M.; Schulz, R. E.; Lork, E. *Z. Anorg. Allg. Chem.* **1998**, *624*, 81.
- (14) Althaus, H.; Breunig, H. J.; Lork, E. *Organometallics* **2001**, *20*, 586.
- (15) Nunn, M.; Begley, M. J.; Sowerby, D. B.; Haiduc, I. *Polyhedron* **1996**, *15*, 3167.
- (16) Breunig, H. J.; Denker, M.; Ebert, K. H. *J. Organomet. Chem.* **1994**, *470*, 87.
- (17) Breunig, H. J.; Borrmann, T.; Lork, E.; Rat, C. I. *J. Organomet. Chem.* **2007**, *692*, 2593.
- (18) Brown, M. D.; Levason, W.; Reid, G.; Webster, M. *Dalton Trans.* **2006**, 4039.
- (19) (a) Copolovici, D.; Bojan, V. R.; Rat, C. I.; Silvestru, A.; Breunig, H. J.; Silvestru, C. *Dalton Trans.* **2010**, *39*, 6357. (b) Soran, A.; Silvestru, C.; Breunig, H. J.; Balazs, L.; Green, J. C. *Organometallics* **2007**, *26*, 1196. (c) Yasuike, S.; Kishi, Y.; Kawara, S.; Yamaguchi, K.; Kurita, J. *J. Organomet. Chem.* **2006**, *691*, 2213. (d) Opris, L. M.; Preda, A. M.; Varga, R. A.; Breunig, H. J.; Silvestru, C. *Eur. J. Inorg. Chem.* **2009**, 1187. (e) Opris, L. M.; Silvestru, C.; Breunig, H. J.; Lork, E. *Dalton Trans.* **2003**, 4367.

- (20) Kakusawa, N.; Tobiyasu, Y.; Yasuike, S.; Yamaguchi, K.; Seki, H.; Kurita, J. *J. Organomet. Chem.* **2006**, *691*, 2953.
- (21) (a) Benjamin, S. L.; Karagannides, L.; Levason, W.; Reid, G.; Rogers, M. C. *Organometallics* **2011**, *30*, 895. (b) Benjamin, S. L.; Levason, W.; Reid, G.; Rogers, M. C. *Dalton Trans.* **2011**, *40*, 6565.
- (22) (a) Chiffey, A. F.; Evans, J.; Levason, W.; Webster, M. *Organometallics* **1996**, *15*, 1280. (b) Jura, M.; Levason, W.; Reid, G.; Webster, M. *Dalton Trans.* **2009**, 7811.
- (23) Golic, L.; Milicev, S. *Acta Crystallogr. Sect. B* **1978**, *34*, 3379.
- (24) Bombieri, G.; Bruno, G.; Nicolo, F.; Alonzo, G.; Bertazzi, N. *J. Chem. Soc., Dalton Trans.* **1987**, 2451.
- (25) Breunig, H. J.; Borrmann, T.; Lork, E.; Moldovan, O.; Rat, C. J.; Wagner, R. P. *J. Organomet. Chem.* **2009**, *694*, 427.
- (26) (a) Buchner, W.; Schenk, W. A. *Inorg. Chem.* **1984**, *23*, 132. (b) Bodner, G. M.; May, M. P.; McKinney, L. E. *Inorg. Chem.* **1980**, *19*, 1951.
- (27) Holmes, N. J.; Levason, W.; Webster, M. *J. Chem. Soc., Dalton Trans.* **1998**, 3457.
- (28) Bojan, V. R.; Fernandez, E. J.; Laguna, A.; Lopez-de-Luzuriaga, J. M.; Monge, M.; Olmos, M. E.; Puellas, R. C.; Silvestru, C. *Inorg. Chem.* **2010**, *49*, 5530.
- (29) See web-site: [www.ccdc.cam.ac.uk/products/csd/radii/](http://www.ccdc.cam.ac.uk/products/csd/radii/) for values used by the CCDC and literature references. Cordero, B.; Gómez, V.; Platero-Prats, A. E.; Revés, M.; Echeverria, J.; Cremades, E.; Barragán, F.; Alvarez, S. *Dalton Trans.* **2008**, 2832.
- (30) Uson, R.; Riera, V.; Gimeno, J.; Laguna, M.; Gamasa, M. P. *J. Chem. Soc., Dalton Trans.* **1979**, 996.
- (31) Holmes, N. J.; Levason, W.; Webster, M. *J. Organomet. Chem.* **1998**, *568*, 213.
- (32) (a) Breunig, H. J.; Althaus, H.; Rosler, R.; Lork, E. *Z. Anorg. Allg. Chem.* **2000**, *626*, 1137. (b) Levason, W.; Matthews, M. L.; Reid, G.; Webster, M. *Dalton Trans.* **2004**, 51.
- (33) Strohmeier, W. *Angew. Chem.* **1964**, *76*, 873.
- (34) Sheldrick, G. M. *SHELXS-97, Program for Crystal Structure Solution*; University of Göttingen: Germany, 1997.
- (35) Sheldrick, G. M. *SHELXL-97, Program for Crystal Structure Refinement*; University of Göttingen: Germany, 1997.